Intermittent Aeration Suppresses Nitrite-Oxidizing Bacteria in Membrane-Aerated Biofilms: A Model-Based Explanation

Ma, Yunjie; Domingo Felez, Carlos; Plósz, Benedek G.; Smets, Barth F.

Published in:
Environmental Science and Technology

Link to article, DOI:
10.1021/acs.est.7b00463

Publication date:
2017

Document Version
Peer reviewed version

Environmental Science & Technology

Article

pubs.acs.org/est

Suppression of Nitrite-Oxidizing Bacteria in Intermittently Membrane-Aerated Biofilms: A Model-Based Explanation

Yunjie Ma, Carlos Domingo-Félez, Benedek Gy. Plósz,† and Barth F. Smets*

Department of Environmental Engineering, Technical University of Denmark, Miljøvej Building 113, 2800 Kongens Lyngby, Denmark

Supporting Information

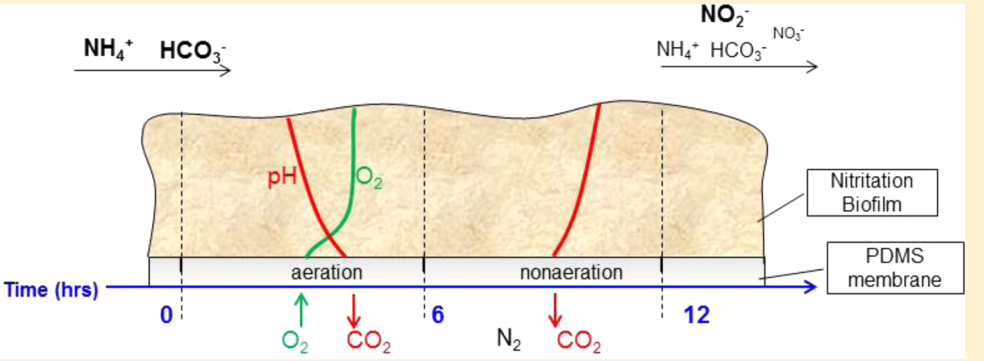

ABSTRACT: Autotrophic ammonium oxidation in membrane-aerated biofilm reactors (MABRs) can make treatment of ammonium-rich wastewaters more energy-efficient, especially within the context of short-cut ammonium removal. The challenge is to exclusively enrich ammonium-oxidizing bacteria (AOB). To achieve nitritation, strategies to suppress nitrite-oxidizing bacteria (NOB) are needed, which are ideally grounded on an understanding of underlying mechanisms. In this study, a counter-diffusion nitrifying biofilm reactor was operated under intermittent aeration. During eight months of operation, AOB dominated, while NOB were suppressed. On the basis of dissolved oxygen (DO), ammonium, nitrite, and nitrate profiles within the biofilm and in the bulk, a 1-dimensional nitrifying biofilm model was developed and calibrated. The model was utilized to explore the potential mechanisms of NOB suppression associated with intermittent aeration, considering DO limitation, direct pH effects on enzymatic activities, and indirect pH effects on activity via substrate speciation. The model predicted strong periodic shifts in the spatial gradients of DO, pH, free ammonia, and free nitrous acid, associated with aerated and nonaerated phases. NOB suppression during intermittent aeration was mostly explained by periodic inhibition caused by free ammonia due to transient periodic pH upshifts. Dissolved oxygen limitation did not govern NOB suppression. Different intermittent aeration strategies were then evaluated for nitritation success in intermittently aerated MABRs: both aeration intermittency and duration were effective control parameters.

1. INTRODUCTION

Short-cut ammonium (NH_4^+) removal via nitrite (NO_2^-) is more energy- and cost-efficient than traditional NH_4^+ removal via nitrate (NO_3^-) due to reduced aeration and external electron donor requirements.[1−3] This process requires full nitritation (oxidation of all NH_4^+ to NO_2^-) and zero nitratation (oxidation of none of the NO_2^- to NO_3^-): in other words, minimal activity of nitrite-oxidizing bacteria (NOB) and maximal activity of ammonium-oxidizing bacteria (AOB). Similar conditions, with only partial nitritation, can also be exploited to convert NH_4^+ to a 50:50 mixture of NO_2^- and NH_4^+, which can then be coupled to anoxic NH_4^+ oxidation to attain even more resource efficient ammonium removal.[4,5]

Various conditions have been successfully tested to suppress NOB over AOB activity or wash-out NOB over AOB biomass to attain nitritation in suspended growth systems. They include the operation of bioreactors at limited dissolved oxygen (DO) concentrations,[6] at high temperature combined with low solids retention times,[1] and at elevated free ammonia (FA) and/or free nitrous acid (FNA) concentrations.[7] In all cases, NOB suppression or outcompetition versus AOB is based on differential growth kinetics. Sometimes, the proper choice of system inoculum also accelerates AOB over NOB selection.[8] In contrast, maintaining long-term nitritation in biofilm-based reactors can be more challenging[9] due to long solids retention times in biofilms that interfere with outcompetition based on kinetic principles. Finding operational conditions and confirming mechanisms that suppress NOB in biofilms remain a challenge. On the one hand, the existence of strong spatial chemical gradients (e.g., of DO, pH, and nitrogenous species) in nitrifying biofilms[10] makes it difficult to prescribe environ-

Received: January 24, 2017
Revised: April 26, 2017
Accepted: April 27, 2017
Published: April 27, 2017

DOI: 10.1021/acs.est.7b00463
Environ. Sci. Technol. XXXX, XXX, XXX−XXX

mental conditions that favor AOB over NOB in the system. On the other hand, the existence of multiple simultaneous chemical gradients complicates identification of the underlying mechanism(s) that suppresses NOB. For example, pH and DO gradients occur simultaneously in active nitrifying biofilms:[11] it is difficult to unravel to what extent nitritation failure or success is associated with the differential effect of oxygen (AOB and NOB having different oxygen affinities)[12] or the differential effects of pH (AOB and NOB responding differently to pH, as a consequence of the pH-dependent maximum growth rates[13,14] and the pH-dependent speciation of FA and FNA which act as both substrates and inhibitors).

Mathematical models are one way to describe multiple processes that occur simultaneously in time and space in nitrifying biofilms.[15,16] A multispecies nitrifying biofilm model (MSNBM) was explicitly developed to study the competition between AOB and NOB; effects of DO, pH, FA, and FNA on growth kinetics were incorporated in a spatially explicit way to evaluate operational conditions for NOB suppression in codiffusion biofilms.[3,17] Park et al.[17] showed that FA inhibition of NOB was more efficient in nascent biofilms (when residual NH_4^+ was still high), but that DO limitation was the dominant mechanism of NOB suppression in established biofilms. Besides bulk DO and influent NH_4^+ concentration, the model suggested that bulk buffer capacity was another means to manipulate NOB suppression by affecting pH gradients within biofilms.

While AOB/NOB competition in conventional codiffusion biofilms has been studied in some detail,[3,17,18] there are less studies on AOB/NOB competition in the context of nitritation in counter-diffusion biofilms. Counter−diffusion biofilms develop in membrane-aerated biofilm reactors (MABRs), where air delivery is via the biofilm base.[19] MABRs have been broadly explored for autotrophic N removal.[11,20,21] In counter-diffusion nitrifying MABRs, active bacteria thrive at the base of the biofilm, where they utilize oxygen supplied from the membrane lumen. Growth of bacteria, including NOB, at the biofilm base would limit the chance for outcompetition, once established, due to spatial protection by the overlying biofilm layers. Efficient operation of MABRs to attain long-term nitritation has, to our knowledge, not been documented, with the exception of one, highly loaded (33 g-N/m^2/day), fully NH_4^+ penetrated MABR where controlling DO concentrations at the membrane−biofilm interface sufficed to maintain nitritation.[22]

Recently, Pellicer-Nàcher et al.[21] observed that fully nitratated MABRs accumulated NO_2^- immediately after switching from continuous to intermittent aeration, even at elevated oxygen loadings. The causal link between nitritation onset and aeration regime change was not explored. Here, we report additional experimental evidence of NOB suppression in intermittently aerated MABRs and we develop and calibrate an improved MSNBM incorporating explicit pH calculation. Using the calibrated model, we systematically evaluate potential causes for NOB suppression associated with intermittent aeration. From this analysis, we identify the periodic FA inhibition, caused by transient pH upshifts and decreases at the biofilm base, as the likely key cause for NOB suppression. A suitable operational window for an effective nitritation control in counter-diffusion systems is finally proposed.

2. MATERIALS AND METHODS

2.1. Reactor Operation and Measurement Methods. *2.1.1. Reactor Configuration and Operation.* The counter-diffusion MABRs consisted of two tubular gas filled PDMS membranes (3100506, Labmarket, Germany), both fixed in parallel to their longer dimension (Figure S1). The system had a liquid volume of 0.83 L (reactors: 31.5 × 5 × 3.5 cm) and was inoculated with enriched nitrifying biomass.[21] To start up the system, the reactor was first run in a batch mode with an initial NH_4^+ concentration at 300 mg-N/L and continuous aeration. The onset of NH_4^+ consumption without oxygen accumulation in the bulk suggested biomass attachment around the membranes. Subsequently, the MABR was operated in continuous flow mode under intermittent aeration. Synthetic wastewater was fed continuously with an NH_4^+ concentration at 75 mg-N/L and without external organic carbon. Hydraulic retention time was 12 h. The intermittent aeration strategy consisted of a 6 h aeration period (100% air) followed by a 6 h nonaeration period (100% N_2). The aeration cycles were controlled by a set of solenoid valves, and the pressure in the lumen was 35 kPa. The bulk phase was completely mixed by recirculating at 1.5 L/min. DO and pH were measured with electrodes in the recirculation line (CellOX 325 and Sentix 41, WTW, Germany). Bulk pH was not controlled and remained at 7.2 ± 0.2 due to adequate buffer capacity (molar ratio in the influent: HCO_3^-/NH_4^+ = 2.1). Reactor temperature was at 32.5 ± 0.7 °C, which was above ambient temperature due to the unintentional heat added by the recirculation pump. The working temperature was not controlled to a lower value, as temperature effect on nitritation success in MABRs is minor.[23,24] N concentrations (NH_4^+, NO_2^-, and NO_3^-) were measured with colorimetric test kits (Spectroquant 14776, 00683, 09713; Merck, Germany).

2.1.2. Microelectrode Measurements. Commercially available DO microelectrode (OX-10, Unisense, Denmark) and lab-made potentiometric microelectrodes for NH_4^+, NO_2^-, and NO_3^-[25] were used for in situ profiling measurements within the biofilm. Profiling measurements were performed after biofilms reached steady state. Microelectrodes were controlled by a motorized micromanipulator to a precision up to 10 μm and began from the top of the biofilm. During measurements, the influent and recirculation were kept unchanged. For each profile, replicates ($n > 3$) were made and the average was considered in model fitting. Besides calibration following the protocols, the signal drift of N-species sensors over time was corrected by measuring N concentrations from effluent before and after profiling.

2.2. Model Development. The MSNBM is a one-dimensional model based on Terada et al.,[26] incorporating additional explicit pH calculation (Table S1). It was implemented in AQUASIM V2.1 with two compartments: a completely mixed gas compartment and a biofilm compartment containing biofilm and bulk liquid.[27] In the counter-diffusion regime, a physical diffusion link connects the gas compartment to the base of the biofilm, defined as

$$A \times k_{M,i}\left(\frac{1}{H_i}C_{i,air} - C_{i,base}\right) \quad (1)$$

where $C_{i,air}$ and $C_{i,base}$ are concentrations of carbon dioxide (CO_2) or oxygen (O_2) in the gas compartment and at the biofilm base (mg/L), H is the nondimensional Henry's Law coefficient (1.32 for CO_2, 34.55 for O_2, 33 °C), and $k_{M,i}$ is the

DOI: 10.1021/acs.est.7b00463
Environ. Sci. Technol. XXXX, XXX, XXX−XXX

silicone membrane gas mass transfer coefficient (k_{M,O_2} = 6 m/d, k_{M,CO_2} = 0.8 m/d, Table S3). Gas transfer of N_2 and NH_3 is not modeled. Other major modeling assumptions, regarding biofilm structure, diffusion mass transfer, and boundary layer thickness, are as in Terada et al.[26] Process rate expressions are shown in Table S2. The calibrated nitrification model incorporating pH is available from the corresponding author.

2.2.1. Biological Processes. The MSNBM includes 3 active microbial groups, AOB, NOB, and heterotrophs (HB), and inerts accumulated during decay processes. For the two-step nitrification process, FA and FNA are considered as true substrates for growth and inhibition in nitritation and nitratation.[28] The growth rate expressions are described as follows,

$$\text{AOB: } \mu_{AOB} \times X_{AOB} \times \frac{S_{O_2}}{K_{O_2}^{AOB} + S_{O_2}} \times \frac{S_{FA}}{K_{FA}^{AOB} + S_{FA} + S_{FA} \times S_{FA}/K_{I,FA}^{AOB}} \times \frac{K_{I,FNA}^{AOB}}{K_{I,FNA}^{AOB} + S_{FNA}} \quad (2)$$

$$\text{NOB: } \mu_{NOB} \times X_{NOB} \times \frac{S_{O_2}}{K_{O_2}^{NOB} + S_{O_2}} \times \frac{S_{FNA}}{K_{FNA}^{NOB} + S_{FNA} + S_{FNA} \times S_{FNA}/K_{I,FNA}^{NOB}} \times \frac{K_{I,FA}^{NOB}}{K_{I,FA}^{NOB} + S_{FA}} \quad (3)$$

where μ is the specific growth rate coefficient (1/day), dependent on local pH and μ_{max}; S_{O_2}, S_{FA}, and S_{FNA} are O_2, FA, and FNA concentrations (mg/L), respectively; K_{O_2}, K_{FA}, and K_{FNA} are half-saturation coefficients (mg/L); $K_{I,FA}$ and $K_{I,FNA}$ are inhibition coefficients (mg/L). Growth substrate inhibition (FA for AOB, FNA for NOB) is incorporated with the Andrews equation. Other types of inhibition (FA for NOB, FNA for AOB) are described with a noncompetitive inhibition term, as routinely done in similar studies.[28,29]

For the denitrification process, NO_2^- and NO_3^- are modeled as separate electron acceptors. To avoid unnecessary complexity and focus on AOB/NOB competition, no intermediates (NO or N_2O) are considered. Bacteria have different decay rates in aeration and nonaeration periods: to simplify the model, AOB/NOB are assumed not to decay under anoxic or anaerobic conditions;[30] meanwhile, HB decay is modified by an anoxic reduction factor during nonaeration periods.

2.2.2. Chemical Process: pH Calculation. The one-dimensional model can keep track of local pH changes perpendicular to the membrane substratum. pH along biofilm depth is calculated on the basis of the proton production via nitrification and consumption via denitrification, the equilibrium reaction with bicarbonate buffer, and CO_2 stripping to the membrane lumen. The consumption of inorganic carbon for autotrophic growth is neglected as it has insignificant influence on pH changes under conditions when inorganic carbon is not limiting.

Protons produced and consumed in bioprocesses are listed in the stoichiometry matrix. The acid–base balance reaction with bicarbonate buffer is assumed to occur much faster than biological processes.[31]

$$H^+ + HCO_3^- \leftrightarrow H_2CO_3(CO_2) \quad \text{rate:} \left(\frac{S_{HCO_3^-} \times S_H}{K_{a,HCO_3}} - S_{CO_2}\right) \times 10^7 \quad (4)$$

where S_H, $S_{HCO_3^-}$, and $S_{H_2CO_3(CO_2)}$ are concentrations of proton, bicarbonate, and the sum of carbonic acid and dissolved carbon dioxide, respectively (μmol/L); K_{a,HCO_3} is the dissociation equilibrium constant of carbonic acid (0.574 μmol/L, 33 °C, 1 atm). Protons produced in the nitritation process titrate HCO_3^- to H_2CO_3, and oversaturated CO_2 diffuses from the biofilm base to the membrane lumen (eq 1). Acid–base reactions with phosphate ions were minor and neglected, as the molar ratio of $H_2PO_4^-/HCO_3^-$ in influent was lower than 3%.

2.2.3. Limitations/Inhibitions of AOB/NOB Activity. The growth rate expressions of AOB and NOB consider DO and pH effects. DO limitation is assessed by oxygen affinity constants. Two pH effects are included. (1) pH–enzyme effect: pH can affect nitrifying activity directly by changing the enzyme reaction mechanism or increasing the demand for maintenance energy.[31,32] A Gaussian bell-shaped curve is chosen to model the pH–enzyme dependency of specific growth rates.[13]

$$\mu = \frac{\mu_{max}}{2}\left\{1 + \cos\left[\frac{\pi}{\omega} \times (pH - pH_{opt})\right]\right\} \quad |pH - pH_{opt}| < \omega \quad (5)$$

where μ_{max} is the maximum specific growth rate at the optimal pH, pH_{opt}, and ω is the pH range within which μ is larger than a half of μ_{max}; (2) pH substrate-speciation effect: local pH values determine FA/FNA speciation from total NH_4^+/NO_2^-. The speciation between ionized/un-ionized species is assumed at instantaneous equilibrium.[33]

$$S_{FA} = \frac{K_{a,NH_3} \times S_{NH_4}}{S_H} \quad S_{FNA} = \frac{S_{NO_2} \times S_H}{K_{a,NO_2}} \quad (6)$$

where K_{a,NH_3} and K_{a,NO_2} are dissociation equilibrium constants of ammonium and nitrous acid, respectively (0.000794 and 628.96 μmol/L (33 °C, 1 atm)). Substrate speciation will result in differential degrees of FA/FNA inhibition.

2.3. Sensitivity Analysis and Parameter Estimation. To investigate the most determinant parameters on reactor performance, a sensitivity analysis was performed. Initial values of kinetic parameters were taken from the ASMN model.[28] The optimal pH ranges for AOB and NOB growth kinetics (pH_{opt} and ω) were from Park et al.[13] The temperature correction for μ_{max} and b_{max} are from Hao et al.[34] The MSNBM was first run in continuous aeration with default values for 300 days to achieve a stable nitrifying biofilm. Then, a local sensitivity analysis was performed after switching to intermittent aeration, giving the individual parameter a 100% value change while all others remained constant.[27] Reactor performances were evaluated in terms of ammonium removal efficiency (ARE, $\frac{S_{NH_4,in} - S_{NH_4,eff}}{S_{NH_4,in}}$%), nitrate production efficiency (NaE, $\frac{S_{NO_3,eff}}{S_{NH_4,in} - S_{NH_4,eff}}$%), nitritation efficiency (NE, $\frac{S_{NO_2,eff}}{S_{NH_4,in} - S_{NH_4,eff}}$%) and NOB fraction (fNOB, $\frac{NOB}{NOB + AOB}$%). The normalized sensitivity function is defined as,

$$\delta_j = \sqrt{\text{average}(\text{Sens}_{i,j}^2)} \text{ and } \text{Sens}_{i,j} = p_{i,j}\frac{\Delta y_j}{\Delta p_{i,j}} \quad (7)$$

DOI: 10.1021/acs.est.7b00463
Environ. Sci. Technol. XXXX, XXX, XXX–XXX

where δ_j, y_j, and $p_{i,j}$ are the sensitivity function, the output reactor performances (ARE, NaE, NE, or fNOB), and the input parameters, respectively. $Sens_{i,j}$ was evaluated at different times during the aeration cycles (time interval of 0.01 day) and at 20 equidistant points within the biofilm or 1 point in the bulk phase. The averaged value was considered in the sensitivity analysis, and parameter sensitivity was ranked for each targeted performance metric. We focused on biokinetic and stoichiometric parameters related to AOB and NOB, as HB parameters are of secondary importance in nitrifying biofilms.[35]

The most sensitive parameters were calibrated with steady state experimental data. The model calibration was carried out by trial and error through adjusting the parameter values one by one to minimize the fitting error. Root mean squared error was used to assess the quality of model-data fit as the objective function,

$$\mathrm{RMSE} = \sqrt{\mathrm{average}\left(\sum_j \sum_i \left(\frac{y_{\mathrm{model},i,j} - y_{\mathrm{meas},i,j}}{y_{\mathrm{meas},j,\mathrm{average}}}\right)^2\right)} \quad (8)$$

where j is the targeted variable measured or estimated (NH_4^+, NO_2^-, NO_3^-, and DO) and i is a sample point along biofilm depth (i = 20). The model was validated with additional experimental data from this MABR and experimental data from a separate membrane-aerated biofilm reactor (MABR2) operated under 4 different ammonium surface loadings (Table S5, detailed description of the experimental data used in model calibration and validation).[36] The calibrated parameters were checked by comparing RMSE in the calibration with RMSE in the validation and the Janus coefficient (J) was calculated,[37]

$$J^2 = \frac{\mathrm{RMSE}_{\mathrm{val}}{}^2}{\mathrm{RMSE}_{\mathrm{cal}}{}^2} \quad (9)$$

2.4. Model Simulations. The calibrated MSNBM was run in 3 scenarios (Table S6, detailed description of each simulation scenario):

(1) To validate the model with extra experimental data, the calibrated MSNBM was ran in intermittent aeration (6 h aeration period and 6 h nonaeration period) under different NH_4^+ surface loadings or in continuous aeration in a batch test. Then, the determinant factor(s) that govern NOB suppression in this MABR was explored with the validated model.

(2) To clarify why NOB suppression occurred after switching to intermittent aeration from continuous aeration, the model was run in continuous aeration to achieve a nitrifying biofilm; then, aeration was switched to the same intermittent aeration as scenario 1.

(3) To optimize the operational window for nitritation in intermittently aerated MABRs, different intermittent aeration strategies and influent concentrations were simulated in MSNBM after achieving a nitrifying biofilm in continuous aeration. The effects of aeration intermittency and residual NH_4^+ (FA) concentrations on NOB suppression were evaluated.

3. RESULTS AND DISCUSSION

3.1. Model Calibration and Evaluation. A sensitivity function, considering the sum of reactor performances (ARE, NaE, NE, and fNOB), was calculated to rank parameters (Figure S2). The most sensitive parameter is μ_{max}^{AOB}, followed by $K_{I,FA}^{AOB}$, μ_{max}^{NOB}, $K_{I,FA}^{NOB}$, $K_{O_2}^{AOB}$, and $K_{O_2}^{NOB}$. The ranking shows that μ_{max} is the most determinant among all kinetic parameters in nitrogen conversion simulations. It is consistent with the sensitivity analysis of Wang et al.[35] who ranked kinetic parameters in terms of nitritation performance and biofilm development in nitrifying biofilm reactors. The higher sensitivity regarding performance within the biofilm (Figure S2B) versus the bulk (Figure S2A) suggests that in situ microprofiling data is more informative in model calibration than bulk measurements, which were typically used.[22,38] Therefore, microprofiling measurements (NH_4^+, NO_2^-, NO_3^-, and DO) in the first aeration hour at steady state were used to calibrate sensitive parameter(s). Microprofiles in the last aeration hour (NH_4^+, NO_2^-, NO_3^-, and DO) and bulk profiles during an intermittent aeration cycle (NH_4^+, NO_2^-, NO_3^-, DO, and pH) representing the reactor performance at steady state were used for validation. Additional validation of the model and its parameter estimates was obtained by fitting the initial reactor performance (NH_4^+, NO_2^-, and NO_3^-) when operated in batch start-up mode and by fitting the biofilm performance (NH_4^+, NO_2^-, NO_3^-, and pH) of a separately operated MABR under different NH_4^+ surface loadings.

By fitting the most sensitive parameter, μ_{max}^{AOB}, in the reported range,[12] the RMSE decreased to 0.5 and the deviation in NO_3^- fitting contributed the most to the error. Thus, the next most sensitive parameter, μ_{max}^{NOB}, in NO_3^- sensitivity ranking (Figure S3) was added to the calibration and RMSE decreased to 0.1. Values of μ_{max}^{AOB} and μ_{max}^{NOB} were within a reasonable range: the estimated maximum growth rates at the optimal pH were 2.35 d^{-1} for AOB and 2.15 d^{-1} for NOB (Table 1). In the data fitting, the error function was bounded, but μ_{max}^{AOB} and μ_{max}^{NOB} were highly correlated indicating a poorly identifiable parameter set. Model evaluations were, however, not affected by changes in the μ_{max}^{AOB} (2.35−2.85) and μ_{max}^{NOB} (2.15−2.55) best-fit parameter value region (Figure S3D, approximate >99% confidence region: μ_{max}^{AOB}, 2.25−2.95; μ_{max}^{NOB}, 2.06−2.66). Predicted microprofiles agree with measurements in the first aeration hour at steady state (Figure 1A): NH_4^+ is consumed along biofilm depth and NO_2^- is produced; NO_3^- remains at lower concentrations than NO_2^- within the biofilm; DO penetrates 60 μm into the biofilm base. The greatest divergence

Table 1. Kinetic Parameter Values of AOB and NOB in the Calibrated Model

kinetic parameters	AOB	NOB	references
μ_{max}: the maximum specific growth rate, 1/d	2.35 (2.72[a])	2.15 (1.75[a])	this study
K_{O_2}: half-saturation coefficient for O_2, mg/L	0.6	1.2	Hiatt and Grady[28]
Y: autotrophic yield, mgCOD/mgN	0.18	0.06	Hiatt and Grady[28]
K_{FA}^{AOB}, K_{FNA}^{NOB}: half-saturation coefficient, mg/L	0.0075	0.0001	Hiatt and Grady[28]
$K_{I,FA}$: free ammonia inhibition coefficient, mg/L	1	0.2	Hiatt and Grady[28]
$K_{I,FNA}$: free nitrous acid inhibition coefficient, mg/L	0.1	0.04	Hiatt and Grady[28]
b_{max}: decay coefficient, 1/d	0.17	0.073	Hao et al.[34]
pH_{opt} (ω): optimal pH	8.4(3.2)	7.7(2.4)	Park et al.[13]

[a]Default growth rates in ASMN with temperature correction (33 °C).

DOI: 10.1021/acs.est.7b00463
Environ. Sci. Technol. XXXX, XXX, XXX−XXX

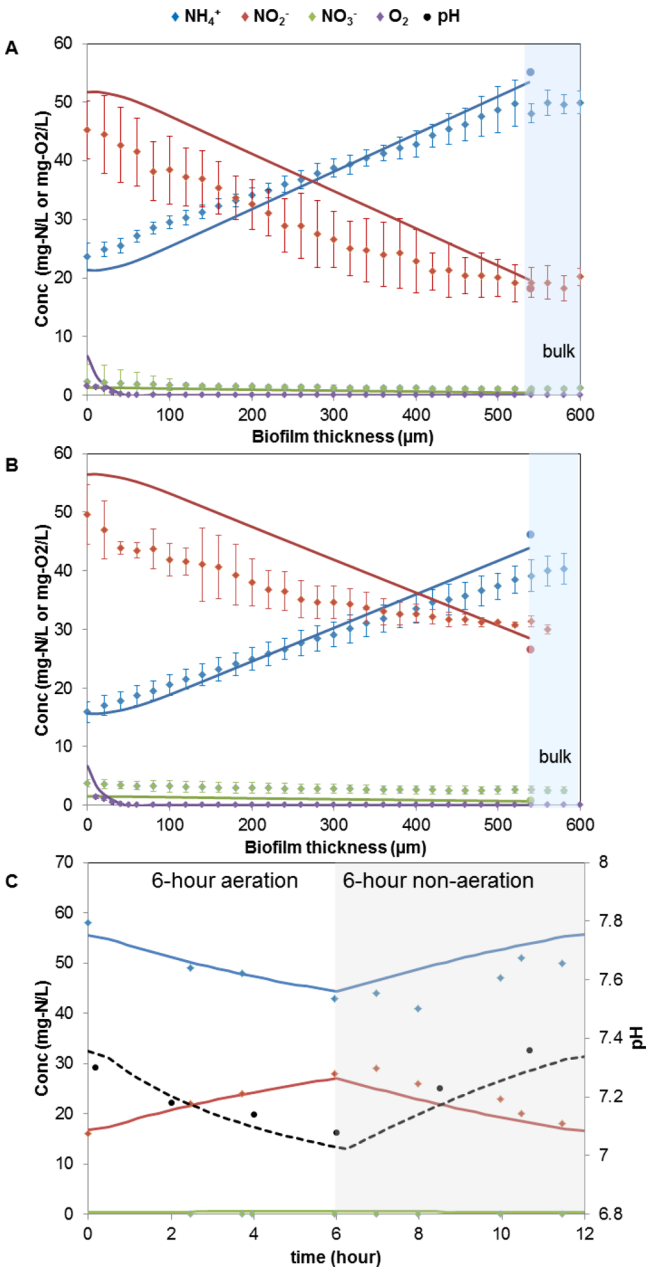

Figure 1. Experimental (discrete symbols) and predicted (line) concentrations in MABR at steady state (A) microprofiles in the first aeration hour, (B) microprofiles in the last aeration hour, and (C) bulk profiles during a 12 h intermittent aeration cycle. For each microprofile, replicates ($n > 3$) were made and the average was shown.

in the overall fitting corresponds to NO_2^- at the biofilm base (6 mg-N/L) but only overestimates FNA concentrations by 0.002 mg-N/L. Errors in DO fitting at the membrane−biofilm interface (6.6 mg/L predicted versus 1.7 mg/L measured) have a minor influence on the oxygen competition between AOB and NOB (Table S4), consistent with Lackner and Smets[39] who reported that oxygen concentrations at interfaces were not decisive in nitritation performance in MABRs. Additionally, uncertainty in measuring the interface DO could be caused by microbial activities on the membrane and an efficiency factor E (1.3−4.3) was suggested to correct measured values.[36]

MSNBM predicts consistent profiles in the different model validations. It predicted lower NH_4^+ and higher NO_2^- within the biofilm in the last aeration hour (Figure 1B) and uniform dynamic variations of bulk concentrations during a 12 h intermittent aeration cycle. For example, it captured the pH decreases in the 6 h aeration phase and increases in the 6 h nonaeration phase (Figure 1C). It also predicted simultaneous production of NO_2^- and NO_3^- in the batch mode data validation (Figure S4A) and predicted NH_4^+ consumption and NO_2^- production following the tendencies observed in MABR2 (Figure S4B). Janus coefficients were around 1.9 (±0.5), showing that the RMSEs were within the same order of magnitude in calibration and validations.

3.2. Model-Based Exploration of NOB Suppression in Intermittently Aerated MABRs. NOB suppression is the result of indirect and direct (competitive) interactions between AOB and NOB in the local environment. Net microbial activities are captured in the specific growth rates: biomass types with the higher specific growth rate will win the local competition. In the studied system, oxygen was provided intermittently from membrane lumen. The biomass type with the higher specific growth rate (AOB or NOB) thus dominated the oxygen utilization.

Consistent with experimental reactor operations, simulations were initiated with fully nitrifying biomass and subject to intermittent aeration. Both simulation and experimental data showed that after 2 weeks in intermittent aeration bulk N concentrations became stable, especially NO_3^- was below 1 mg-N/L indicating efficient suppression of NOB activity (Figure S9). To illustrate the competition in the first nitrifying stage, profiles of specific growth rates of AOB and NOB during an aeration cycle (6 h) are plotted at day 15 (Figure 2A). The averaged μ at time intervals shows kinetic variations over time: (1) 0−15 min, with the onset of aeration microbial activities recover from the previous nonaeration period and increase dramatically; (2) 15−180 min, AOB activity becomes stable, while NOB activity still recovers; (3) 180−360 min, both AOB and NOB activity reach pseudosteady state. The model shows the ratio of μ_{AOB} to μ_{NOB} increases in the intermittent aeration, compared to the ratio of μ_{max}^{AOB} to μ_{max}^{NOB} in continuous aeration (1.5 ± 0.15 versus 1.1). AOB preferentially utilize oxygen to support growth while NOB are outcompeted or their activity is suppressed.

To assess the relative contribution of DO/pH effects on NOB suppression, individual factors influencing growth rates were calculated spatially (at different biofilm depths) and temporally (at different times during the cycle). Considering the effective DO penetration depth, only results in the first 100 μm at the biofilm base are shown (Figure 2B).

3.2.1. DO Limitation in NOB Suppression. O_2 is a growth substrate for both AOB and NOB. In counter-diffusion biofilms, O_2 is provided via the lumen and NH_4^+ via the bulk. In the biofilm, DO penetrates only 60 μm during aeration periods with the highest concentration at the membrane−biofilm interface (biofilm depth= 0 μm), presenting spatial variations (Figure S5A). Besides, DO varies over time during aeration cycles. DO at the membrane−biofilm interface is 0 mg/L at the onset of aeration and quickly increases to the maximum concentration within 15 min. Afterward, DO concentrations within the biofilm remain stable until the end of aeration.

The DO limitation effect was evaluated on the basis of oxygen concentrations within the biofilm (Figure 2B, 1, DO limitation). In aeration periods, during the first 15 min, DO strongly limits both AOB and NOB activities. During the

DOI: 10.1021/acs.est.7b00463
Environ. Sci. Technol. XXXX, XXX, XXX−XXX

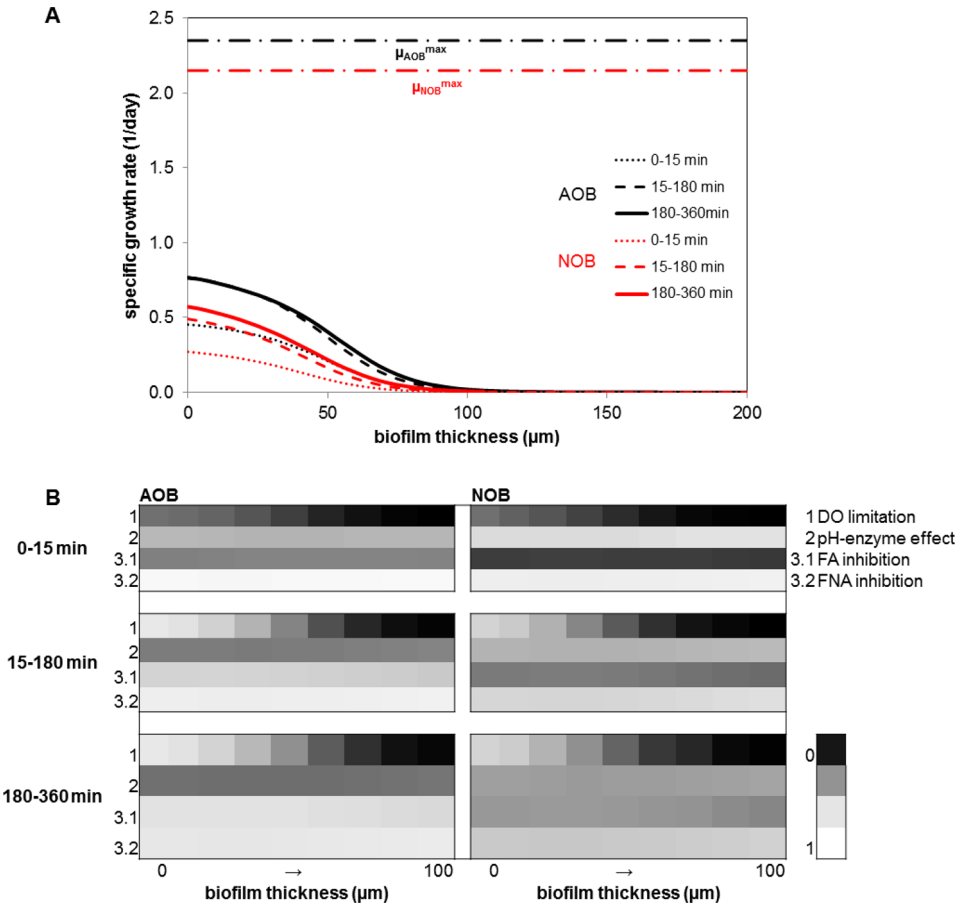

Figure 2. (A) Specific growth rates of AOB and NOB within the biofilm in a 6 h aeration period at day 15 (AOB, black; NOB, red). (B) Individual effect on AOB and NOB within the 100 μm-aerated biofilm base in a 6 h aeration period at day 15 (0, strong limitation/inhibition effect; 1, no limitation/inhibition effect).

following period, the limitation is alleviated as DO increases and stabilizes but still remains strong above 30 μm. With a lower DO affinity. NOB are more oxygen-limited than AOB. However, the relatively stronger limitation to NOB is insignificant in its suppression. Model results show that oxygen transfer and its diffusion mostly affects NH_4^+ oxidation efficiency rather than nitritation efficiency (Table S7).

3.2.2. pH−Enzyme Effect on NOB Suppression. Because pH affects AOB/NOB kinetics directly and indirectly, it is necessary to incorporate pH effects in models.[14,40] Here, MSNBM predicts local pH values within the biofilm and the response to transient aeration phases (Figure S5B). While measurements showed that bulk pH remained relatively stable (±0.2), pH within the biofilm, especially in the DO-penetrated zone, showed considerable variations (±0.6). At the onset of aeration, the model indicates a transient pH upshift at the biofilm base (0−15 min). The accumulated alkalinity is attributed to continuous CO_2 diffusion from the biofilm base to the membrane lumen where N_2 gas flows through in the previous nonaeration period and slight denitrification activities. As aeration continues, pH decreases due to proton production associated with NH_4^+ oxidation. Simulations predict that pH within the biofilm becomes lower than in the bulk after 1 h of aeration and decreases slowly afterward. At the end of aeration, pH at the biofilm base is 0.4 units lower than the average bulk pH, which will increase again in the following nonaerated phase. Thus, pH varies periodically in the intermittently aerated biofilms, a pattern similar but slower than DO variations.

The pH−enzyme effect was assessed on the basis of local pH values (Figure 2B, 2, pH−enzyme effect). It favors NOB growth over AOB as NOB have a lower pH_{opt} (NOB: 7.7 versus AOB: 8.4) and pH varies in the optimal range for its growth. Moreover, the pH−enzyme effect is also insignificant in the overall AOB/NOB competition due to their robust growth in broad pH ranges and the relatively small pH variations in the system.

3.2.3. pH Substrate-Speciation Effects on NOB Suppression. FA/FNA concentrations rely on pH values as well as total NH_4^+/NO_2^- concentrations. In counter-diffusion biofilms, NH_4^+, provided via the bulk, is oxidized at the biofilm base producing NO_2^- which diffuses backward into the bulk.[10] On the basis of ionic N concentrations, FA and FNA speciation synchronizes with pH variations (Figure S5C,D). For instance, at the onset of aeration, FA concentration is high due to NH_4^+ and alkalinity accumulation from the previous nonaeration period. During the following aeration period, FA concentration decreases, as pH drops and NH_4^+ consumption continues. On the other hand, FNA shows reversed variations: increasing as aeration progresses and with biofilm depth as a result of the proton and NO_2^- production.

The pH substrate-speciation effect was assessed on the basis of FA/FNA concentrations within the biofilm (Figure 2B, 3, FA/FNA inhibition). During the first 15 min, FA strongly inhibits AOB/NOB microbial activities (FA > $K_{I,FA}$). Afterward, the inhibition is alleviated as FA decreases. Noticeably, FA inhibits AOB and NOB in different ways: the inhibition effect

DOI: 10.1021/acs.est.7b00463
Environ. Sci. Technol. XXXX, XXX, XXX−XXX

Table 2. Predicted Nitritation Efficiencies (NE, %) in Various Intermittent Aeration Strategies

	influent[b]		effluent (bulk)			
simulation case	NH_4^+ (mg-N/L)	buffer capacity[b]	NH_4^+ (mg-N/L)	pH	FA[c] (mg-N/L)	$NE_{normalized}$[d]
continuous	75	2.1	39	6.96	0.27	0.01
A: 6 + 6[a]	75	2.1	53.0 ± 5	7.23 ± 0.15	0.71	1.00[d]
B: 1 + 1	75	2.1	52.5 ± 1	7.22 ± 0.02	0.69	0.73
C: 12 + 12	75	2.1	53.1 ± 10	7.25 ± 0.25	0.78	0.79
D: 8 + 4	75	2.1	47.8 ± 4	7.14 ± 0.15	0.52	0.41
E: 6 + 6	100	2.1	72.0 ± 7	7.25 ± 0.15	1.02	1.74
F: 6 + 6	50	2.1	35.0 ± 3	7.20 ± 0.15	0.45	0.21
G: 6 + 6	50	5	31.2 ± 5	7.41 ± 0.10	0.64	0.83

[a]Aeration strategy 6 + 6 meant a 12 h intermittent aeration cycle consisting of a 6 h aeration phase and a 6 h nonaeration phase. [b]Buffer capacity in the influent was recorded as the molar ratio of bicarbonate (HCO_3^-) to ammonium (NH_4^+_N). [c]FA was calculated with the averaged NH_4^+ concentrations and bulk pH during a full aeration cycle (eq 6). [d]For a clear comparison, NE was normalized to the nitritation efficiency in the default simulation case A (NE = 48.5%). MSNBM was run in continuous aeration (200 days) to achieve a mature nitrifying biofilm, followed by various intermittent aeration strategies: (A–D) different intermittent aeration but the same influent; (A, E–G) the same aeration intermittency but different influent concentrations. NEs in the NOB suppression process in intermittent aeration were recorded (e.g., at day 215) (Table S6). In simulations E–G, oxygen loadings proportionally varied with NH_4^+ influent concentrations (more simulations in Table S8).

remains strong for NOB throughout the aeration period (from 0.26 to 0.62), while it obviously weakens for AOB (from 0.54 to 0.89). FA inhibition rapidly becomes the most determinant factor in suppressing NOB over AOB. As FNA concentrations are always an order of magnitude lower than $K_{I,FNA}$, its inhibition effect on microbial activities is always minor thereby contributing little to NOB suppression.

Besides the inhibitor effect ($K_I/(K_I + S)$), FA/FNA exhibit the substrate limitation effect ($S/(K_S + S)$) in biological processes (eq 2). However, FA and FNA concentrations are far above the substrate affinities (K_{FA}^{AOB} and K_{FNA}^{NOB}) in the system, making the substrate limitation effects negligible.

3.2.4. Implication of Model-Based NOB Suppression. Overall, FA inhibition caused by pH substrate speciation is the crucial factor in suppressing NOB in the intermittently aerated biofilm reactors. Nitritation success is insensitive to oxygen affinity constants or DO concentrations at the membrane–biofilm interface, a conclusion different from previous studies.[41,42] Downing and Nerenberg[22] suggested manipulating interface DO as an effective method to control shortcut nitrification in MABRs: with a lower interface DO, more NO_2^- accumulated. However, their biofilms performed at low nitrification rates with a low influent NH_4^+ concentration, 3 mg-N/L, suggesting little FA inhibition and no NO_2^- accumulation or significant pH gradients. The single DO gradient within the biofilm presents the interface DO as having a key role in nitritation success. This method might not apply for N-rich wastewater treatment. For example, Lackner and Smets[39] concluded that nitritation success based only on interface DO was not possible in a counter-diffusion biofilm with high influent NH_4^+ concentrations (20–800 mg-N/L), and nitritation efficiency was not predicted from oxygen affinity constants.

Counter- and codiffusion biofilms have different mechanisms of NOB suppression due to different spatial structures and population distributions.[35,38,39] In counter-diffusion biofilms, the theoretically optimal habitat for NOB is the biofilm base, where both S_{O_2}/K_{O_2} and S_{FNA}/K_{FNA} have the highest values. In contrast, the base is not the optimal for AOB growth, as S_{O_2}/K_{O2} and S_{FA}/K_{FA} cannot have the maximum at the same spatial position. Outcompeting NOB can be more difficult in counter-diffusion over codiffusion biofilms, where microbes (AOB and NOB) share the optimal habitats at the biofilm top near the biofilm/liquid interphase. Others have similarly observed that NOB could survive better in counter- versus codiffusion biofilms, even when operated under constant oxygen limited (DO < 0.1 mg/L) and high pH (8.0–8.3) conditions in the bulk.[35] The inherent system geometry of membrane-aerated biofilms complicates NOB inhibition/washout. Besides, when applying intermittent aeration, periodic pH variations at the biofilm base exert a significant effect on NOB dynamics in counter-diffusion biofilms because of continuous CO_2 diffusion to the gas lumen. However, such pH variations are not expected in codiffusion biofilms. Many studies have highlighted the benefits of low DO with high FA to maintain shortcut NH_4^+ removal in codiffusion biofilms.[17,43] Park et al.[3] explored simultaneous effects of DO and FA/FNA in lab-scale codiffusion nitrifying biofilms and found that NO_2^- accumulated due to DO limitation or FA inhibition and long-term NOB suppression could not be maintained without DO limitation involved. The results were consistent with Brockmann and Morgenroth[44] who suggested that oxygen limitation was the main mechanism for NOB suppression and FA inhibition was not necessarily required in codiffusion biofilms. However, DO limitation in nitritation counter-diffusion biofilms appears not as significant as reported for codiffusion biofilms, consistent with the observation that nitritation could not be achieved by solely manipulating air pressure in the membrane lumen in MABRs.[21]

3.3. Potential Explanation of NOB Suppression in the Study of Pellicer-Nàcher et al.[21] To answer why NO_2^- accumulated after switching from continuous to intermittent aeration in MABRs, simulations were carried out with the calibrated MSNBM in continuous aeration for 200 days followed by intermittent aeration (6 h aeration and 6 h nonaeration cycles). The simulation shows a nitrifying biofilm during continuous aeration (NE = 0%) indicating no NOB suppression (Table 2, continuous aeration). After switching to intermittent aeration, the model predicts NOB suppression: NO_3^- decrease and NE increase (Table 2- strategy A, Figure S6). To find the critical factor for NOB suppression, variations of the individual pH/DO effect on AOB/NOB competition were assessed: each effect $\frac{effect_{AOB}}{effect_{NOB}}$ in intermittent aeration (for instance at day 215) was normalized by its value during continuous aeration. A value higher than 1 means the effect

DOI: 10.1021/acs.est.7b00463
Environ. Sci. Technol. XXXX, XXX, XXX–XXX

favors NOB suppression in intermittent aeration, and a value lower than 1 indicates it favors NOB growth.

Only FA inhibition is identified to favor NO_2^- accumulation after switching the aeration strategy, while DO limitation, pH–enzyme effect, and FNA inhibition remain unchanged (Figure S7). FA inhibition shows certain varying patterns in intermittent aeration: (1) overall, it is enhanced due to an increased residual NH_4^+; (2) it is particularly strong during the first 15 min of aeration. The simulated increase of residual NH_4^+ after changing to intermittent aeration was also observed in the study of Pellicer-Nàcher et al.:[21] in reactor B, bulk NH_4^+ increased by 100 mg/L at stages 1 and 2 (intermittent aeration) compared to stage 0 (continuous aeration). Compared to continuous aeration, MABRs in intermittent aeration display a trade-off between NH_4^+ removal efficiency and nitritation efficiency (Table 2). Nitritation is assisted by the evaluated residual NH_4^+, which underlines the importance of a minimum NH_4^+ concentration in the bulk. Pérez et al.[18] also highlighted the need for minimum residual NH_4^+ for NOB suppression in codiffusion biofilms but attributed the nitritation success to differential oxygen limitation rather than FA inhibition, as NOB were outcompeted due to the strong oxygen limiting conditions imposed by a high residual NH_4^+. The strong FA inhibition at the onset of aeration is due to pH upshifts at the biofilm base in the previous anoxic phases. It causes a longer lag phase of NOB activity over AOB, which could be another reason for the nitritation success. Theoretically, NOB locate at the biofilm base, if enriched in MABRs; thus, pH upshift at the base is more efficient to prompt FA inhibition than increasing bulk pH. This lag phase has also been observed in other intermittently aerated systems.[45,46] Kornaros et al.[47] and Gilbert et al.[48] attributed the lag phase to a long (enzyme) reactivation time in NOB nitrogen metabolism after anoxic exposure in batch continuous stirred-tank reactors. However, the possibility for pH variations was not considered in those studies, even though CO_2 stripping could slowly increase bulk pH.[49]

3.4. Nitritation in Various Intermittent Aeration Strategies. For an intermittent aeration system with certain NH_4^+/O_2 surface loadings, the aeration duration determines residual NH_4^+ concentrations: a longer aeration lowers residual NH_4^+. The aeration intermittency determines pH upshift times and the variation range of bulk concentrations: a higher frequency causes more pH upshifts and a narrow variation range. This information can be utilized to optimize intermittent aeration strategies for efficient nitritation in MABRs (Table 2). MSNBM simulation shows that a higher aeration intermittency can accelerate NOB suppression (A and C) due to more times of pH upshift in nonaeration phases to retard NOB activity while slightly affecting AOB activity or decelerate NOB suppression (B and A) due to the relatively high bulk NH_4^+ (pH) at the onset of aeration phases even though the averaged bulk concentrations are the same. Longer aeration duration (D) leads to a slower nitritation process but a higher NH_4^+ removal efficiency, while keeping the same aeration intermittency. It is consistent with the observation in Mota et al.[50] that intermittently aerated reactors with longer anoxic phase had the lower NOB abundance and relatively higher NH_4^+ effluent concentrations. Both studies suggest that the maximum aeration duration should be set to ensure nitritation success in intermittent aeration, and a specific to the treated wastewater ratio of aeration to nonaeration phase is needed to balance NOB suppression against NH_4^+ removal.[51] Simulation with high NH_4^+ concentrations predicts fast nitritation in the intermittent aeration (E) and vice versa slow nitritation with low influent NH_4^+ (F). Further simulation with low NH_4^+ concentrations but high bulk pH (G) shows efficient nitritation, confirming a key factor in NOB suppression was bulk FA rather than residual NH_4^+ (more simulations in Table S8). In an intermittent aeration regime, the bulk FA can provide a rapid indicator of the nitritation potential of MABRs (Figure S10). MSNBM simulations reveal that aeration duration and intermittency control the performance of intermittently aerated nitrifying biofilms: longer aeration duration ensures a higher NH_4^+ removal efficiency yet impedes NOB suppression; higher aeration intermittency presents unchanged NH_4^+ removal performance, while its effect on NOB suppression should be evaluated under specific conditions. Following this model-based analysis, experimental validation of model predictions is warranted.

In conclusion, we provide experimental evidence that intermittent aeration supports efficient nitritation in membrane aerated biofilm reactors (MABRs). A pH-explicit 1-D multi-species nitrifying biofilm model (MSNBM) is developed and calibrated: model analysis reveals that NOB suppression, associated with intermittent aeration, is primarily governed by *periodic* FA inhibition as the consequence of transient pH upshifts during nonaeration. These pH upshifts are mainly caused by alkalinity increases due to CO_2 stripping to the membrane lumen (which also occurs during aeration) *plus* the cessation of proton production (which only occurs during aeration). In counter diffusion biofilms, pH effect is more important than DO (limitation) effect on NOB suppression. Both aeration intermittency and duration are effective control factors to obtain nitritation success in intermittently membrane-aerated biofilms, and maintaining nitritation and NH_4^+ removal efficiency is more easily ensured if operated with high buffer capacities.

■ ASSOCIATED CONTENT

Supporting Information

The Supporting Information is available free of charge on the ACS Publications website at DOI: 10.1021/acs.est.7b00463.

More detailed information on model description, model simulations, and data analysis (PDF)

■ AUTHOR INFORMATION

Corresponding Author

*E-mail: bfsm@env.dtu.dk; tel: +45 4525 1600; fax: +45 4593 2850.

ORCID

Barth F. Smets: 0000-0003-4119-6292

Present Address

†B.G.P.: Department of Chemical Engineering, University of Bath, Claverton Down, BA2 7AY Bath, United Kingdom.

Notes

The authors declare no competing financial interest.

■ ACKNOWLEDGMENTS

The authors would like to thank the China Scholarship Council (CSC) for financial support to Y.M. and the Innovation Fund Denmark (IFD) (Project LaGAS, File No. 0603-00523B) for additional financial support.

DOI: 10.1021/acs.est.7b00463
Environ. Sci. Technol. XXXX, XXX, XXX–XXX

REFERENCES

(1) Hellinga, C.; Schellen, A.; Mulder, J.; Vanloosdrecht, M.; Heijnen, J. The sharon process: An innovative method for nitrogen removal from ammonium-rich waste water. *Water Sci. Technol.* **1998**, *37* (9), 135−142.

(2) Jenicek, P.; Svehia, P.; Zabranska, J.; Dohanyos, M. Factors affecting nitrogen removal by nitritation/denitritation. *Water Sci. Technol.* **2004**, *49* (5−6), 73−79.

(3) Park, S.; Chung, J.; Rittmann, B. E.; Bae, W. Nitrite accumulation from simultaneous free-ammonia and free-nitrous-acid inhibition and oxygen limitation in a continuous-flow biofilm reactor. *Biotechnol. Bioeng.* **2015**, *112* (1), 43−52.

(4) van Dongen, U.; Jetten, M. S.; van Loosdrecht, M. C. The SHARON-Anammox process for treatment of ammonium rich wastewater. *Water Sci. Technol.* **2001**, *44* (1), 153−160.

(5) Kuenen, J. G. Anammox bacteria: from discovery to application. *Nat. Rev. Microbiol.* **2008**, *6* (4), 320−326.

(6) Sliekers, A. O.; Haaijer, S. C. M.; Stafsnes, M. H.; Kuenen, J. G.; Jetten, M. S. M. Competition and coexistence of aerobic ammonium- and nitrite-oxidizing bacteria at low oxygen concentrations. *Appl. Microbiol. Biotechnol.* **2005**, *68* (6), 808−817.

(7) Vadivelu, V. M.; Yuan, Z.; Fux, C.; Keller, J. The inhibitory effects of free nitrous acid on the energy generation and growth processes of an enriched Nitrobacter culture. *Environ. Sci. Technol.* **2006**, *40* (14), 4442−4448.

(8) Terada, A.; Lackner, S.; Kristensen, K.; Smets, B. F. Inoculum effects on community composition and nitritation performance of autotrophic nitrifying biofilm reactors with counter-diffusion geometry. *Environ. Microbiol.* **2010**, *12* (10), 2858−2872.

(9) Fux, C.; Huang, D.; Monti, A.; Siegrist, H. Difficulties in maintaining long-term partial nitritation of ammonium-rich sludge digester liquids in a moving-bed biofilm reactor (MBBR). *Water Sci. Technol.* **2004**, *49* (11−12), 53−60.

(10) Schramm, A.; De Beer, D.; Gieseke, A.; Amann, R. Microenvironments and distribution of nitrifying bacteria in a membrane-bound biofilm. *Environ. Microbiol.* **2000**, *2* (6), 680−686.

(11) Shanahan, J. W.; Semmens, M. J. Alkalinity and pH effects on nitrification in a membrane aerated bioreactor: An experimental and model analysis. *Water Res.* **2015**, *74*, 10−22.

(12) Vannecke, T. P. W.; Volcke, E. I. P. Modelling microbial competition in nitrifying biofilm reactors. *Biotechnol. Bioeng.* **2015**, *112* (12), 2550−2561.

(13) Park, S.; Bae, W.; Chung, J.; Baek, S.-C. Empirical model of the pH dependence of the maximum specific nitrification rate. *Process Biochem.* **2007**, *42* (12), 1671−1676.

(14) Fumasoli, A.; Morgenroth, E.; Udert, K. M. Modeling the low pH limit of Nitrosomonas eutropha in high-strength nitrogen wastewaters. *Water Res.* **2015**, *83*, 161−170.

(15) Carrera, J.; Jubany, I.; Carvallo, L.; Chamy, R.; Lafuente, J. Kinetic models for nitrification inhibition by ammonium and nitrite in a suspended and an immobilised biomass systems. *Process Biochem.* **2004**, *39* (9), 1159−1165.

(16) Martin, K. J.; Picioreanu, C.; Nerenberg, R. Assessing microbial competition in a hydrogen-based membrane biofilm reactor (MBfR) using multidimensional modeling. *Biotechnol. Bioeng.* **2015**, *112* (9), 1843−1853.

(17) Park, S.; Bae, W.; Rittmann, B. E. Multi-Species Nitrifying Biofilm Model (MSNBM) including free ammonia and free nitrous acid inhibition and oxygen limitation. *Biotechnol. Bioeng.* **2010**, *105* (6), 1115−1130.

(18) Pérez, J.; Lotti, T.; Kleerebezem, R.; Picioreanu, C.; van Loosdrecht, M. C. M. Outcompeting nitrite-oxidizing bacteria in single-stage nitrogen removal in sewage treatment plants: A model-based study. *Water Res.* **2014**, *66*, 208−218.

(19) Casey, E.; Glennon, B.; Hamer, G. Review of membrane aerated biofilm reactors. *Resour. Conserv. Recycl.* **1999**, *27* (1−2), 203−215.

(20) Terada, A.; Yamamoto, T.; Igarashi, R.; Tsuneda, S.; Hirata, A. Feasibility of a membrane-aerated biofilm reactor to achieve controllable nitrification. *Biochem. Eng. J.* **2006**, *28* (2), 123−130.

(21) Pellicer-Nàcher, C.; Sun, S.; Lackner, S.; Terada, A.; Schreiber, F.; Zhou, Q.; Smets, B. F. Sequential aeration of membrane-aerated biofilm reactors for high-rate autotrophic nitrogen removal: experimental demonstration. *Environ. Sci. Technol.* **2010**, *44* (19), 7628−7634.

(22) Downing, L. S.; Nerenberg, R. Effect of oxygen gradients on the activity and microbial community structure of a nitrifying, membrane-aerated biofilm. *Biotechnol. Bioeng.* **2008**, *101* (6), 1193−1204.

(23) Pellicer-Nàcher, C.; Sun, S.; Lackner, S.; Terada, A.; Schreiber, F.; Zhou, Q.; Smets, B. F. Sequential aeration of membrane-aerated biofilm reactors for high-rate autotrophic nitrogen removal: experimental demonstration. *Environ. Sci. Technol.* **2010**, *44* (19), 7628−7634.

(24) Zhu, S.; Chen, S. The impact of temperature on nitrification rate in fixed film biofilters. *Aquac. Eng.* **2002**, *26* (4), 221−237.

(25) Gieseke, A.; de Beer, D. Use of microelectrodes to measure in situ microbial activities in biofilms, sediments, and microbial mats. *Mol. Microb. Ecol. Man.* **2008**, *2*, 3483−3514.

(26) Terada, A.; Lackner, S.; Tsuneda, S.; Smets, B. F. Redox-stratification controlled biofilm (ReSCoBi) for completely autotrophic nitrogen removal: the effect of co- versus counter-diffusion on reactor performance. *Biotechnol. Bioeng.* **2007**, *97* (1), 40−51.

(27) Reichert, P. *AQUASIM 2.0—Computer program for the identification and simulation of aquatic systems*; EAWAG: Dubendorf, Switzerland, 1998.

(28) Hiatt, W. C.; Grady, C. P. L. An updated process model for carbon oxidation, nitrification, and denitrification. *Water Environ. Res.* **2008**, *80*, 2145−2156.

(29) Hellinga, C.; Van Loosdrecht, M. C. M.; Heijnen, J. J. Model Based Design of a Novel Process for Nitrogen Removal from Concentrated Flows. *Mathematical and Computer Modelling of Dynamical Systems* **1999**, *5*, 351−371.

(30) Blackburne, R.; Yuan, Z.; Keller, J. Demonstration of nitrogen removal via nitrite in a sequencing batch reactor treating domestic wastewater. *Water Res.* **2008**, *42*, 2166−2176.

(31) Sötemann, S.; Musvoto, E.; Wentzel, M.; Ekama, G. Integrated biological, chemical and physical processes kinetic modelling Part 1 − Anoxic-aerobic C and N removal in the activated sludge system. *Water SA* **2006**, *31* (4), 1044−1062.

(32) Van Hulle, S. W. H.; Volcke, E. I. P.; Teruel, J. L.; Donckels, B.; van Loosdrecht, M. C. M.; Vanrolleghem, P. A. Influence of temperature and pH on the kinetics of the Sharon nitritation process. *J. Chem. Technol. Biotechnol.* **2007**, *82* (5), 471−480.

(33) Musvoto, E. V.; Wentzel, M. C.; Loewenthal, R. E.; Ekama, G. A. Integrated chemical-physical processes modelling - I. Development of a kinetic-based model for mixed weak acid/base systems. *Water Res.* **2000**, *34* (6), 1857−1867.

(34) Hao, X.; Heijnen, J. J.; Van Loosdrecht, M. C. Model-based evaluation of temperature and inflow variations on a partial nitrification−ANAMMOX biofilm process. *Water Res.* **2002**, *36* (19), 4839−4849.

(35) Wang, R.; Terada, A.; Lackner, S.; Smets, B. F.; Henze, M.; Xia, S.; Zhao, J. Nitritation performance and biofilm development of co- and counter-diffusion biofilm reactors: modeling and experimental comparison. *Water Res.* **2009**, *43* (10), 2699−2709.

(36) Pellicer-Nàcher, C.; Domingo-Félez, C.; Lackner, S.; Smets, B. F. Microbial activity catalyzes oxygen transfer in membrane-aerated nitritating biofilm reactors. *J. Membr. Sci.* **2013**, *446*, 465−471.

(37) Power, M. The predictive validation of ecological and environmental models. *Ecol. Modell.* **1993**, *68* (1−2), 33−50.

(38) Brockmann, D.; Rosenwinkel, K.-H.; Morgenroth, E. Practical identifiability of biokinetic parameters of a model describing two-step nitrification in biofilms. *Biotechnol. Bioeng.* **2008**, *101* (3), 497−514.

(39) Lackner, S.; Smets, B. F. Effect of the kinetics of ammonium and nitrite oxidation on nitritation success or failure for different biofilm reactor geometries. *Biochem. Eng. J.* **2012**, *69*, 123−129.

(40) Vangsgaard, A. K.; Mauricio-Iglesias, M.; Valverde-Pérez, B.; Gernaey, K. V.; Sin, G. pH variation and influence in an autotrophic

DOI: 10.1021/acs.est.7b00463
Environ. Sci. Technol. XXXX, XXX, XXX−XXX

nitrogen removing biofilm system using an efficient numerical solution strategy. *Water Sci. Technol.* **2013**, *67* (11), 2608.
(41) Wyffels, S.; Van Hulle, S. W. H.; Boeckx, P.; Volcke, E. I. P.; Van Cleemput, O.; Vanrolleghem, P. A.; Verstraete, W. Modeling and simulation of oxygen-limited partial nitritation in a membrane-assisted bioreactor (MBR). *Biotechnol. Bioeng.* **2004**, *86* (5), 531−542.
(42) Volcke, E. I. P.; Sanchez, O.; Steyer, J.-P.; Dabert, P.; Bernet, N. Microbial population dynamics in nitrifying reactors: Experimental evidence explained by a simple model including interspecies competition. *Process Biochem.* **2008**, *43* (12), 1398−1406.
(43) Chung, J.; Bae, W.; Lee, Y.-W.; Rittmann, B. E. Shortcut biological nitrogen removal in hybrid biofilm/suspended growth reactors. *Process Biochem.* **2007**, *42* (3), 320−328.
(44) Brockmann, D.; Morgenroth, E. Evaluating operating conditions for outcompeting nitrite oxidizers and maintaining partial nitrification in biofilm systems using biofilm modeling and Monte Carlo filtering. *Water Res.* **2010**, *44* (6), 1995−2009.
(45) Yoo, H.; Ahn, K.-H.; Lee, H.-J.; Lee, K.-H.; Kwak, Y.-J.; Song, K.-G. Nitrogen removal from synthetic wastewater by simultaneous nitrification and denitrification (SND) via nitrite in an intermittently-aerated reactor. *Water Res.* **1999**, *33* (1), 145−154.
(46) Gilbert, E. M.; Agrawal, S.; Brunner, F.; Schwartz, T.; Horn, H.; Lackner, S. Response of Different Nitrospira Species To Anoxic Periods Depends on Operational DO. *Environ. Sci. Technol.* **2014**, *48* (5), 2934−2941.
(47) Kornaros, M.; Dokianakis, S. N.; Lyberatos, G. Partial Nitrification/Denitrification Can Be Attributed to the Slow Response of Nitrite Oxidizing Bacteria to Periodic Anoxic Disturbances. *Environ. Sci. Technol.* **2010**, *44* (19), 7245−7253.
(48) Gilbert, E. M.; Agrawal, S.; Brunner, F.; Schwartz, T.; Horn, H.; Lackner, S. Response of Different Nitrospira Species To Anoxic Periods Depends on Operational DO. *Environ. Sci. Technol.* **2014**, *48* (5), 2934−2941.
(49) Li, J.; Elliott, D.; Nielsen, M.; Healy, M. G.; Zhan, X. Long-term partial nitrification in an intermittently aerated sequencing batch reactor (SBR) treating ammonium-rich wastewater under controlled oxygen-limited conditions. *Biochem. Eng. J.* **2011**, *55* (3), 215−222.
(50) Mota, C.; Head, M. A.; Ridenoure, J. A.; Cheng, J. J.; de los Reyes, F. L. Effects of Aeration Cycles on Nitrifying Bacterial Populations and Nitrogen Removal in Intermittently Aerated Reactors. *Appl. Environ. Microbiol.* **2005**, *71* (12), 8565−8572.
(51) Kornaros, M.; Marazioti, C.; Lyberatos, G. A pilot scale study of a sequencing batch reactor treating municipal wastewater operated via the UP-PND process. *Water Sci. Technol.* **2008**, *58* (2), 435−438.

DOI: 10.1021/acs.est.7b00463
Environ. Sci. Technol. XXXX, XXX, XXX−XXX